Title

Tracking Mechanical Stress and Cell Migration with Inexpensive Polymer Thin-Film Sensors

Journal

Advanced Materials Interfaces, 10(2)

ISSN

2196-7350

Authors

Finney, Tanner J

Frank, Skye L

Bull, Michael R

et al.

Publication Date

2023

DOI

10.1002/admi.202201808

Peer reviewed

HHS Public Access

Author manuscript

Adv Mater Interfaces. Author manuscript; available in PMC 2024 January 17.

Published in final edited form as:

Adv Mater Interfaces. 2023 January 17; 10(2): . doi:10.1002/admi.202201808.

Tracking Mechanical Stress and Cell Migration with Inexpensive Polymer Thin-Film Sensors

Tanner J. Finney,
Department of Chemical Engineering, University of California, Davis, CA 95616, United States

Skye L. Frank,
Department of Chemical Engineering, University of California, Davis, CA 95616, United States

Michael R. Bull,
Department of Chemical Engineering, University of California, Davis, CA 95616, United States

Robert D. Guy,
Department of Mathematics, University of California, Davis, CA 95616, United States

Tonya L. Kuhl
Department of Chemical Engineering, University of California, Davis, CA 95616, United States

Abstract

Polydiacetylene (PDA) Langmuir films are well known for their blue to red chromatic transitions in response to a variety of stimuli, including UV light, heat, bio-molecule bindings and mechanical stress. In this work, we detail the ability to tune PDA Langmuir films to exhibit discrete chromatic transitions in response to applied mechanical stress. Normal and shear-induced transitions were quantified using the Surface Forces Apparatus and established to be binary and tunable as a function of film formation conditions. Both monomer alkyl tail length and metal cations were used to manipulate the chromatic transition force threshold to enable discrete force sensing from ~50 to ~500 nN μm^{-2} for normal loading and ~2 to ~40 nN μm^{-2} for shear-induced transitions, which are appropriate for biological cells. The utility of PDA thin-film sensors was demonstrated with the slime mold *Physarum polycephalum*. The fluorescence readout of the films enabled: the area explored by *Physarum* to be visualized, the forces involved in locomotion to be quantified, and revealed novel puncta formation potentially associated with *Physarum* sampling its environment.

Graphical Abstract

tlkuhl@ucdavis.edu .

[8]Supporting Information

Supporting Information is available from the Wiley Online Library or from the author.

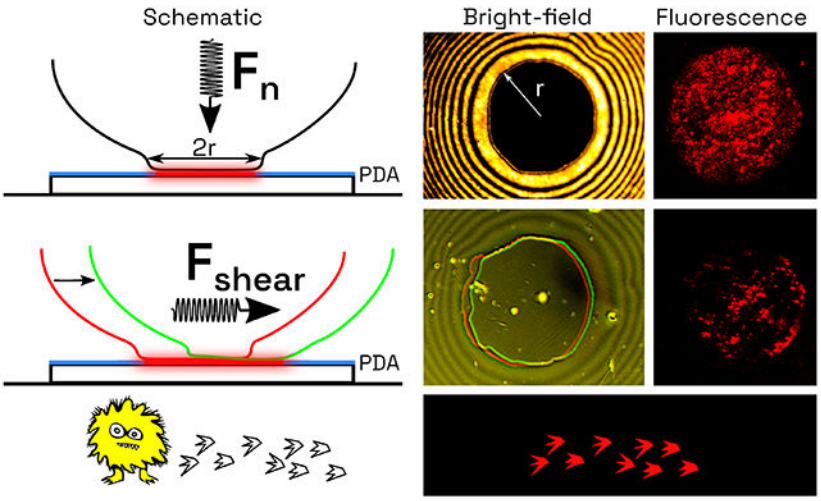

Polydiacetylene thin films fluoresce in response to applied normal and lateral stress. The stress required is quantitative and can be tuned based on film formation conditions. TPDA thin-film sensors were then applied to measure the stresses applied during *Physarum polycephalum* (slime mold) migration.

Keywords

Polydiacetylenes; Cell migration; Mechanochromism; Slime Mold; Surface Forces Apparatus

1 Introduction

Polydiacetylenes are a class of linear polymers that exhibit binary chromatic (blue to red) transitions. PDAs can be self-assembled into Langmuir films and vesicles from various diacetylene (DA) surfactants (Supplemental S1). Exposure of the assembly to UV light induces topochemical polymerization creating a linear conjugated backbone consisting of alternating double and triple bonds [1]. This polymer is visibly blue and non-fluorescent. When exposed to external stimuli such as mechanical stress, heat or UV light, blue phase PDA can undergo a chromatic transition to a visibly red, fluorescent phase (Figure 1b). This chromatic transition has been described as a shift in conjugation caused by torsion of the polymer backbone but is still not fully elucidated and under active theoretical and experimental investigation [2, 3, 4, 5, 6, 7, 8, 9]. Mechanically induced blue-to-red transitions or mechanochromism in PDA Langmuir films was first described by Carpick et al. in several notable articles [10, 11, 12, 13]. It was found that mechanochromism occurred preferentially in the direction of the polymer backbone within a given PDA domain. Subsequently, Juhasz et al. quantitatively described AFM-tip induced mechanochromism using lateral force microscopy [14] but were unable to induce transitions by applying normal force. More recent developments in other modes of mechanochromism in other material forms of PDAs were reviewed by Das et al. [2].

Of interest here is applying the unique properties of PDA mechanochromism to examine the behavior and migration of microorganisms and cells. Techniques to measure the

forces involved in cell migration are often either qualitative or highly complex [15]. We demonstrate the utility and ease of use of PDA thin-film sensors using the model organism, *Physarum polycephalum*. a slime mold. *P. polycephalum* has attracted significant interest in a variety of disciplines due to its ease of culturing, cytoplasmic streaming, ameboid locomotion, and unique demonstration of "intelligence" in maze solving and other demonstrations of cognition [16, 17, 18, 19]. In the plasmodium phase of its lifecycle, it is highly migratory and exerts measurable shear forces. The traction forces of *Physarum* microplasmodia have been examined previously using traction force microscopy (TFM) [20, 21, 22, 23]. *Phyarsum* was observed to exert stresses on the order of magnitude of 100 Pa, with a maximum of ~ 400 Pa. TFM enables high resolution, granular measurements of the forces exerted by cells. Conversely, the work presented here represents a passive, ensemble-level view of the forces and migration exerted by larger slime molds, based entirely on the fluorescent transitions of PDAs.

The mechanochromatic transitions of PDA Langmuir films of different compositions were precisely quantified using a modified Surface Forces Apparatus (SFA) coupled to a polarized epi-fluorescent microscope. PDA films of increasing blue to red transition threshold were fabricated and characterized with the SFA and then applied to examine the locomotion and migration of *Physarum polycephalum*. The SFA is an ideal tool for examining mechanochromism of PDA as the contact area is directly viewable and the fluorescent response to an applied force can be measured in real time. We observed that PDA films exhibited two different sensing modalities, normal stress induced transitions and shear stress induced transitions. These binary transitions occurred only when stress above the transition threshold of the film was applied. This enables applied stresses to be directly viewed through the fluorescence of the PDA film in real time or at some later time point to reveal the mechanical stress footprint. This work details the methodology to produce well-characterized PDA films with known transition properties. The PDA sensing films were then applied to the locomotion of *Physarum* revealing that the slime mold exhibits a range of forces that can be segmented and identified by using films with different mechanical stress thresholds.

2 PDA Film Calibration

2.1 Normal Stress Induced Mechanochromism

The effects of normal stress on PDA mechanochromism have not been previously investigated. Atomic force microscopy studies have shown that PDA mechanochromism can be induced by lateral forces, but were unable to induce transitions by applying normal force [12, 14]. As determined in this work, the normal stress required to induce the blue-to-red transition is orders of magnitude higher than with shear stress. Using a modified SFA coupled with a fluorescent microscope we were able to simultaneously apply normal force, monitor the contact area and, fluorescent readout. For these measurements, a PDA film was deposited onto one SFA disk, and a 20 μm silicone film (a common biological model) was deposited onto the other surface. The silicone film uniformly distributed the normal force and acted as a model of an adhesive substrate, such as a cell. The experimental setup is represented schematically in Figure 1a. The two disks were brought into contact, loaded, and

allowed to equilibrate for 10 minutes. This process was repeated at different positions with increasing load until the contact area was fully transformed from blue (non-fluorescent) to red (highly fluorescent). Figure 1b shows the difference in absorbance and emission spectra between the blue phase (Figure 1c) and mechanically transformed red phase PDA (Figure 1d). Initially, the film is almost entirely in the blue phase. During loading, domain edges and holes begin to fluoresce first, Figure 1c, followed by the bulk transformation of the film within the contact area, Figure 1d. Unlike shear induced transitions, normal stress induced transitions appear to transform the film without a directional dependence relative to the PDA domain orientation (aligned polymer backbone). Importantly, the transformed area does not propagate from the locally loaded area. Furthermore, normal stress mechanochromism was observed to occur from micro to macro length scales; compare Figure 1c,d, and insets.

This calibration method was applied to PDA films formed from DAs of increasing alkyl tail lengths ranging from ECDA, C21 to NCDA, C29. The results of these experiments are summarized in Figure 2. Both the normal stress to transform the bulk film as well as stress to transform the edges and holes of the film domains follow the same trend. The difference between the bulk and edge transformation becomes more pronounced for polymer films made from DA monomers with longer alkyl tails. The UV dose required to induce the blue-to-red transition was compared to normal stress induced transitions. The dose and normal stress followed similar trends; higher doses of UV light or pressure were required to fully induce the blue-to-red transition in DA films with longer alkyl tails [24]. Interestingly, when Zn and Fe were added to the Langmuir trough subphase, the resulting PDA films were found to be unable to undergo normal stress induced transitions within the range applied by the SFA (the maximum normal stress applied in these experiments was approximately 700 $nN\ \mu m^{-2}$).

When in contact with a surface, but below the critical normal stress described above, PDA films are still in the blue phase, and hence non-fluorescent. As described next, these films can be sheared to induce the blue to red transition. This enables two different sensing modes for PDA films: a normal stress sensor at relatively higher loads and a shear stress sensor at zero or lower loads.

2.2 Shear Stress Induced Mechanochromism

The SFA was utilized to measure shear stress induced transitions in PDA films [25]. The experimental design is represented schematically in Figure 3a. The PDA film was brought into contact with a thin silicone film and sheared with zero applied load at different shearing rates and displacements. The shearing velocity was targeted to be on of the order of microns per hour, as to approximate the migration of cellular locomotion [20, 26]. Films sheared with rates between 1 Hz and 100 μHz yielded similar friction forces and fluorescent response. To precisely quantify the shear force, the conditions under which shear induced transformation occurred were first mapped out with the fluorescent coupled SFA and then carefully replicated using a standard SFA configuration, which can precisely measure shear force [25, 27]. Combined with the contact area, critical shear stress was calculated. Below this critical shear stress, films can be repeatedly sheared without any measurable increase in fluorescence. An increase in DA monomer alkyl length leads to an increase in the

critical shear stress required for a transformation, as indicated in Figure 4. The increase in mechanochromism induced by shear stress agrees well with previous observations of the effect of DA alkyl tail length on normal stress transitions, UV dose and thermal transition temperature required to induce the blue to red transition. Van der Waals interactions and hydrogen bonding between neighboring monomers increase as alkyl tail length increases, hence we hypothesize that this increase in van der Waals attraction and hydrogen bonding increases the stimulus necessary to induce the blue-to-red transition [7, 28, 29, 30].

Shear induced mechanochromism is also anisotropic [11, 14]. PDA domains are formed from aligned polymer backbones. PDA backbones that align with the direction of shearing transform at lower shear stresses than those perpendicular or offset from the direction of sliding. The direction of PDA backbones can be observed using polarized light microscopy. Films formed from TCDA (C23) exhibit massive polymer domains, often as large as $0.1mm^2$, while films formed from DAs with longer alkyl tails have domains typically between 10 and 100 μm^2 [24]. Figure 3b shows a transformed TCDA contact region where the entire area of contact was contained within a single domain, and the shear direction was aligned with the orientation of the domain.

Conversely, in Figure 3c, with small PCDA domains, only the domains aligned with the sliding direction transformed. While in Figure 3d, most of the very small NCDA domains were off aligned resulting in relatively small fluorescent patches within the contact area. Large domains in conjunction with polarized light microscopy provide additional avenues for improving stress sensing resolution, as the direction and magnitude of applied stresses may be measured. Conversely, using fabrication methods to obtain ultra-small domains homogenizes the sensor, as described next.

Domain size and the shear stress required for the blue-to-red transition can be strongly modified by adding metal cations during film formation, providing an independent means for tuning the characteristics of the PDA film [24, 31, 32, 33, 34]. Our previous work characterized the effect of metal cations on UV light induced blue to red transitions [24]. Building upon this work, the mechanochromism of Fe-PCDA and Zn-PCDA were investigated. Modifying films with Fe or Zn decreases the domain size and increases the stimulus (normal stress, shear stress or UV Dose) required to transform the film (Figure 4).

Zn modified films exhibit additional novel behavior. Zn-PDA films lack UV photochromism: UV light polymerizes the film to the blue phase, but additional UV light is unable to transform the film to the red phase. Zn-PDA films demonstrate: strong reversible thermochromism at temperatures < 200°C, but the fluorescence is inhibited when thermally transformed [24, 31, 32]. When sheared, Zn-PCDA films undergo the blue to red transition with fluorescence, Figure 5. We hypothesize that shearing disrupts the Zn^{2+} bridging bidentate complexes between neighboring carboxylic acid head groups [24, 31, 34], which enables it to fluorescence similar to a regular film in the absence of Zn^{2+} cations. These strong bridging interactions are responsible for reversible thermochromism and inhibited fluorescence. Hence, Zn cations create a novel sensing modality where shear stress alone can induce fluorescent mechanochromism.

3 Slime Mold Locomotion Induced Mechanochromism

Slime molds, particularly *Physarum polycephalum*, have been extensively studied due to their simplicity, the amoeboid-like behavior of the plasmodium, and their puzzle-solving ability [16, 17, 18, 19, 21, 35]. Low stress threshold ECDA/C21 films were used to examine the migration and document the area explored by *Physarum* as seen in Figure 6a. When a slime mold is placed on a PDA film, migration by the slime mold induces the blue to red transition. Hence, the fluorescent readout indicates every location where the slime mold explored, Figure 6a. A complete record of *Physarum's* migration is captured on the film as the fluorescence is permanent. This is useful because slime molds move relatively slow, less than 0.5 mm h^{-1}, and avoid light (negative phototaxis) [23, 36, 37, 38]. PDA films offer a simple and effective means for passive, non-invasive, long-term surveillance.

PDA films with different stress activation thresholds can distinguish some different potentially shear-applying methods of *Physarum*. Low stress threshold ECDA/C21 (2.1 ± 0.5 nN μm^{-2}) films display a range of fluorescent intensity after slime mold migration, Figure 6a. Shear stresses from the spreading plasmodium and veins were the primary driver of high fluorescence in ECDA/C21 films. Diffuse fluorescence from the spreading plasmodium, bright fluorescent spots and small dark holes of removed film or "puncta" can all be seen. The brighter, more intense fluorescence observed along Figure 6a(i) is likely due to higher stresses exerted by the presence of large vein-like structures over a larger and more uniform region by large vein-like structures. Conversely, diffuse fluorescence is due to small local regions of stress application by the spreading plasmodium. On PCDA and NCDA films with a transition shear stress greater than 4 ± 0.2 nNμm^{-2}, only the localized bright fluorescent spots are present as indicated in Figure 6b and c respectively. These fluorescent spots were potentially from stress fibers and adhesion/anchoring of the organism to the film. Though the slime mold is somewhat autofluorescent, the fluorescence of the PDA film can be observed beneath the organism at the edges (Figure 6b).

The stresses measured in these experiments appear significantly larger than previously measured traction forces with a maximum of ~400Pa as compared to the minimum ~2000 Pa measured here [20, 21, 22, 23]. A significant portion of this discrepancy is due to the scales over which these measurements were taken. TFM studies focused on *Physarum* microplasmodia, where the entire organism was less than ~500 μm in diameter. These microplasmodia appear tubular and lack larger vein-like structures. Here, larger *Physarum* organisms that possessed vein-like structures were studied (See supplemental section S4 for details on slime mold size measurement). While organisms of roughly the same size as the microplasmodia observed in Rieu et al. were examined here, our samples were extracted from *Physarum* macroplasmodia of much larger size. Stockem and Brix extensively described the morphology and structures of both macro and microplasmodia [35, 39, 40, 41]. We speculate that the larger organisms studied here may exhibit higher stresses than those observed by Zhang et al., Rieu et al., and Lewis et al. due to larger, more organized cytoskeletal structures found in macroplasmodia [20, 22, 23, 35]. These larger structures may produce stronger adhesion and migration stresses than those observed in microplasmodia.

Furthermore, measured stresses were observed to scale with the size of the plasmodium. Larger plasmodium sections such as a vein or plasmodium > 100 μm in diameter were observed to induce fluoresce in higher threshold films such as NCDA. In contrast, smaller sections of the plasmodium < 100 μm and the exploring edge of the slime mold could not induce the blue to red transition Figure 7. The “size” of the slime mold was defined by the width of the spreading plasmodium through a given area (See supplemental section S4 for details). Normal stress induced transitions were not considered to be significant contributors to the observed fluorescence of the PDA films. PDA films are an order of magnitude more sensitive to shear stress than normal stress (Figures 2, 4).

In addition to migration induced fluorescence, evidence of slime mold migration stems from the observation of “puncta” or dark holes carved out from the film by the slime mold. As the slime mold advances into a region, these puncta indicia were present throughout the plasmodium and leading edge of the slime mold. The puncta were highly circular and distinguishable from any cracks or defects in the PDA Films, which typically follow polymer domain boundaries (Figure 8). We speculate that this is a potentially unrecognized mechanism by which the slime mold samples or senses the local environment. By using films with a high transformation shear stress, the puncta could be readily identified without the added complications of migration induced fluorescence. This can be seen in Figures 6c and 7, where inside, and just outside the slime mold, the film is covered in puncta, indicating the plasmodium had migrated over that region. In the higher stress threshold NCDA film, figure 6c, the film is littered with puncta, but there is minimal fluorescence from the migrating slime mold. Figure 8 shows the difference between cracks in the PDA film and puncta.

Larger slime mold plasmodium with veins and a size greater than 250 μm were observed to produce larger puncta in the film than smaller spreading plasmodium lacking veins, Figure 9. Fluorescence around the edges of the puncta indicated the film was ripped and detached by the slime mold, as similar ripping induced fluorescence can be seen during SFA experiments when the two disks are rapidly separated.

Based on these experiments, PDA Langmuir films offer a potential new avenue to non-invasively examine migration and related forces of cells and microorganisms. PDA films could potentially be used with mammalian cells and track the movement of fibroblasts and related epithelial cells during a wound healing assay or other biological processes. The carboxylic DA head group is readily functionalizable and could be modified to enhance cell adhesion, detect the presence of biomolecules on the surface of cells, and offer additional avenues to tailor stress sensitivity.

4 Comparison of PDA films to other techniques

PDA thin films may potentially act as more general cell migration sensors. Compared to other techniques for measuring cell migration, PDAs offer several potential advantages. Polacheck and Chen extensively reviewed a number of commonly used cell migration techniques, which have been summarized in Table 1 [42]. PDA based cell migration sensors potentially can image thousands of cells, as PDA films can be uniformly deposited over 10s

of cm^2, with imaging limited only by the field of view of the microscope (Table 1, note b). The stress range and sensitivity of PDAs may be further enhanced by depositing PDAs onto more compliant, elastic materials (Table 1, note d).

PDA films may offer high spatial resolution of exerted forces. Carpick et al. and Juhasz et al. examined mechanochromism of PDA Langmuir films at the nanometer scale. They observed that mechanochromism induced by an AFM tip is viewable with wide-field fluorescence microscopy. Hence, forces exerted on the sub-micrometer scale may be readily observed due to the localized fluorescence of the red phase PDA(Table 1, note c).

The primary advantages of PDA films lie in that the precursor diacetylenes are inexpensive, and the fluorescence left by mechanical stress is permanent and generally irreversible. Requiring only a standard fluorescent microscope, this permanent, non-photobleaching fluorescence potentially allows for passive monitoring of cell migration without the continuous use of a fluorescent microscope. PDA films are not without challenges. Other more compliant substrates need to be evaluated, the cytotoxicity and compatibility of PDAs with other cells has not been thoroughly examined, and the range of stress sensitivities could be improved and refined through head-group functionalization, and deposition onto more elastic substrates.

5 Conclusions

2D mechanical stress sensors with high sensitivity can be easily made from PDA Langmuir films. The binary readout of the films blue-to-red / non-fluorescent to fluorescent transformation provides a simple readout of mechanical stress in real time or to record stress events for later examination. PDA films are sensitive to both normal and lateral stress induced transitions, with significantly higher sensitivity to lateral stress. Importantly the mechanical stress threshold can be readily tuned by modifying film formation parameters. Increasing the monomer alkyl tail length or incorporation of divalent salts into the film can dramatically increase the critical stress required to induce the blue to red transition. Low transition threshold PDA films can be exploited to examine the locomotion and migration of single cells and micro-organisms as demonstrated using the model organism *Physarum polycephalum*, or slime mold. Furthermore, the forces exerted by *Physarum* during locomotion were assessed quantitatively and previously unreported behavior was observed. PDA thin-film sensors are a straightforward method for examining the stresses involved in cell migration and movement in other systems of interest.

6 Experimental Section

6.1 Preparation of PDA Langmuir Films

Our technique for fabricating high-quality PDA Langmuir films has been described previously [24]. 10,12 heneicosadiynoic acid (C21, ECDA) [57], 10,12-tricosadiynoic acid (C23, TCDA), 10,12-pentacosadiynoic acid (C25, PCDA), 10,12-heptacosadiynoic acid (C27, HCDA), and 10,12-nonacosadiynoic acid (C29, NCDA) were from TCI America and GFS Chemicals. Diacetylene (DA) powders were purified using flash column chromatography. The purified DAs were then dissolved in chloroform at 0.4 mg/mL and

deposited dropwise onto the air-water interface of a Nima 611D Langmuir-Blodgett trough. After equilibration for 20 minutes, the trough was compressed at a rate of 20 cm^2 min^{-1} and exposed to 254 nm UV light for approximately 20% of the optimal blue phase UV dose once a stable trilayer film was formed. Films were then transferred to glass substrates using either an angled Langmuir-Blodgett (LB) technique or Langmuir-Schaefer (LS) technique. Transferred films were then exposed to further UV light to maximize the blue phase prior to SFA experiments. For films formed with Zn and Fe cation subphases, the subphase was stirred continuously. Zn-PCDA films were formed with a concentration of 1 mM $ZnCl_2$ in the subphase, and Fe-PCDA films were formed with a subphase of 0.01 mM $FeCl_3$. Anhydrous zinc chloride ($ZnCl_2$) was from Honeywell Fluka and iron (III) chloride hexahydrate ($FeCl_3$-$6H_2O$) was from Sigma Aldrich. See supplemental S2 for details.

6.2 Surface Forces Apparatus Experiments

A modified SFA Mark II was developed to carry out these experiments. The SFA was mounted underneath a polarized epi-fluorescent microscope with an Andor Zyla 5.5 sCMOS camera and Texas Red filter cube. Unlike the traditional silvered mica substrates used in typical SFA experiments, a PDA Langmuir film was directly deposited onto the cylindrically curved side of a plano-cylindrical glass lens (often referred to as an SFA disk) using the Langmuir-Schaefer technique. An identical disk was covered with a 20 μm silicone film (from Silex Ltd., Wacker Chemie). The silicone film was plasma treated to remove it from the Polyethylene terephthalate (PET) backing sheet, attached to a plastic frame, and then draped onto a UV-ozone treated SFA glass disk. The disks are then placed in specialized mounts in the SFA, one above the other with their cylindrical sides facing each other and their axes perpendicular. The contact area between the two disks is readily viewable through a window at the top of the SFA and measurable with a microscope objective. To measure normal force, the vertical movement of a calibrated spring (attached to one of the disc mounts) is tracked with an encoder. Friction forces were measured using a combined SFA friction setup composed of a bimorph driver and friction device with semiconductor strain gauges (See supplemental S3 for details) [25]. This enables precise application of sliding velocities on the order of 1-10 $\mu m h^{-1}$, similar to the migration rate of cells. Custom control and acquisition software was developed and utilized micro-manager and the pycro-manager interface [58, 59, 60]. This setup enabled observation of the fluorescent response to a well-defined displacement, and in subsequent experiments, measurement of the friction force associated with the fluorescent transformation of the film. Absorbance and emission spectra of the films were captured using a Perkin Elmer LAMBDA 750 UV/Vis/NIR spectrophotometer and a Varian Cary Eclipse fluorescence spectrophotometer.

6.3 Slime mold experiments

Cultures of *Physarum polycephalum* were purchased from Carolina Biological Supply, both as living cultures and sclerotium. *Physarum* was cultured on 2% non-nutrient agar (Sigma Aldrich) and sub-cultured every other day, fed Quaker rolled oats and stored in the dark at 24°C. For experiments with PDA films, a small, less than 1 mm radius, of the slime mold and agar was excised and deposited onto a PDA coated cover-slip. The PDA coverslip was embedded in an agar-coated Petri dish for moisture control. Slime mold migration across a PDA film was imaged with a custom polarized fluorescent microscope with an Andor

Zyla 5.5 sCMOS camera. The size of the slime mold was defined as the width of the spreading plasmodium within a given area. See supplemental section S4 for more details and a schematic of experiments.

6.4 Statistical Analysis

Normal Force Mechanochromism: Normal force induced transitions were identified from continuous observation of applied normal force and fluorescence response of the PDA film. For each monomer with a different alkyl tail length, three samples were evaluated. Each sample provided 5-8 unique positions. The mean and standard deviation from all of these positions are reported in Figure 2. This analysis utilized ImageJ/Fiji and Python using numpy, uncertainties and pint.

Shear Force Mechanochromism: Shear force induced transitions were identified by the continuous acquisition of fluorescence microscopy images and response of the SFA bimoprh (See supplemental section S3 for an example of these results). For each PDA film, 3 independent SFA experiments were carried out. Within each SFA experiment, 5-7 unique positions were accessible. Friction response data was smoothed with a Savitzky-Golay filter. The distance between the sliding plateaus in the friction force were identified using a peak identification routine, which, with calibration corresponds to the friction force measured in the system (See Supplemental S3). The mean and standard deviation of these results are reported in Figure 4. Analysis and error propagation utilized ImageJ/Fiji and Python with numpy, pands, scipy, pint and uncertainties packages.

Slime Molds: Slime mold migration analysis was carried out by periodic imaging of migrating slime molds (See Supplemental Section S4). The size of the migrating plasmodium was measured using ImageJ/Fiji and representative samples were reported in Figures 6,7. Slime mold puncta were characterized using local image thresholding algorithms built into Fiji/ImageJ with manual validation. The distribution of slime mold puncta are reported in Figure 9. The box plot shows the mean, quartiles and minimum and maximum of the measured puncta from 40 unique slime mold migration locations across all film configurations.

Supplementary Material

Refer to Web version on PubMed Central for supplementary material.

Acknowledgments

The authors thank Kevin Yates for initial assistance with slime mold cultures, and Zhongrui Liu for assistance with preparing SFA experiments.

This work was partially supported by NIH R01 HL159993-01 and NIH T32 HL086350.

References

[1]. Wegner Gerhard. Topochemische Reaktionen von Monomeren mit konjugierten Dreifach-bindungen / Tochemical Reactions of Monomers with conjugated triple Bonds. Zeitschrift für Naturforschung B, 24(7):824–832, 2014. doi: 10.1515/znb-1969-0708.

[2]. Das Bratati, Jo Seiko, Zheng Jianlu, Chen Jiali, and Sugihara Kaori. Recent Progress in Polydiacetylene Mechanochromism. Nanoscale, 14(5):1670–1678, 2022. doi: 10.1039/D1NR07129G. [PubMed: 35043814]

[3]. Barisien T, Legrand L, Weiser G, Deschamps J, Balog M, Boury B, Dutremez SG, and Schott M. Exciton spectroscopy of red polydiacetylene chains in single crystals. Chemical Physics Letters, 444(4):309–313, August 2007. doi: 10.1016/j.cplett.2007.07.031.

[4]. Schott Michel. The Colors of Polydiacetylenes: A Commentary. The Journal of Physical Chemistry B, 110(32):15864–15868, August 2006. doi: 10.1021/jp0638437. [PubMed: 16898738]

[5]. Lifshitz Yevgeniy, Golan Yuval, Konovalov Oleg, and Berman Amir. Structural Transitions in Polydiacetylene Langmuir Films. Langmuir, 25(8):4469–4477, April 2009. doi: 10.1021/la8029038. [PubMed: 19366221]

[6]. Li Qing, Wang Yi-Xuan, and Chen Yulan. Unraveling Ultrasonic Stress Response of Nanovesicles by the Mechanochromism of Self-Assembled Polydiacetylene. ACS Macro Lett., 11(1):103–109, January 2022. doi: 10.1021/acsmacrolett.1c00715. [PubMed: 35574789]

[7]. Khanantong Chanita, Charoenthai Nipaphat, Phuangkaew Tinnakorn, Kielar Filip, Traiphol Nisanart, and Traiphol Rakchart. Phase transition, structure and color-transition behaviors of monocarboxylic diacetylene and polydiacetylene assemblies: The opposite effects of alkyl chain length. Colloids and Surfaces A: Physicochemical and Engineering Aspects, 553:337–348, September 2018. doi: 10.1016/j.colsurfa.2018.05.081.

[8]. Choi Yeol Kyo, Lee Sang Yup, and Ahn Dong June. Hyperconjugation-induced chromism in linear responsive polymers. Journal of Materials Chemistry C, 7(42):13130–13138, October 2019. doi: 10.1039/C9TC03204E.

[9]. Ortuso Roberto Diego. Characterisation of Polydiacetylene for the Detection of Forces in Membranes. PhD thesis, University of Geneva, 2019.

[10]. Carpick RW, Sasaki DY, and Burns AR. First Observation of Mechanochromism at the Nanometer Scale. Langmuir, 16(3):1270–1278, February 2000. doi: 10.1021/la990706a.

[11]. Carpick RW, Sasaki DY, and Burns AR. Large friction anisotropy of a polydiacetylene monolayer. Tribology Letters, 7(2):79–85, September 1999. doi: 10.1023/A:1019113218650.

[12]. Carpick Robert W., Sasaki Darryl Y., Marcus Matthew S., Eriksson MA, and Burns Alan R.. Polydiacetylene films: A review of recent investigations into chromogenic transitions and nanomechanical properties. Journal of Physics: Condensed Matter, 16(23): R679–R697, May 2004. doi: 10.1088/0953-8984/16/23/R01.

[13]. Sheth SR and Leckband DE. Direct Force Measurements of Polymerization-Dependent Changes in the Properties of Diacetylene Films. Langmuir, 13(21):5652–5662, October 1997. doi: 10.1021/la962107z.

[14]. Juhasz Levente, Ortuso Roberto D., and Sugihara Kaori. Quantitative and Anisotropic Mechanochromism of Polydiacetylene at Nanoscale. Nano Lett, 21(1):543–549, January 2021. doi: 10.1021/acs.nanolett.0c04027. [PubMed: 33284635]

[15]. Colin-York Huw and Fritzsche Marco. The future of traction force microscopy. Current Opinion in Biomedical Engineering, 5:1–5, March 2018. doi: 10.1016/j.cobme.2017.10.002.

[16]. Nakagaki Toshiyuki, Yamada Hiroyasu, and Tóth Ágota. Maze-solving by an amoeboid organism. Nature, 407(6803):470–470, September 2000. doi: 10.1038/35035159. [PubMed: 11028990]

[17]. Oettmeier Christina, Brix Klaudia, and Döbereiner Hans-Günther. Physarum polycephalum—a new take on a classic model system. Journal of Physics D: Applied Physics, 50(41):413001, September 2017. doi: 10.1088/1361-6463/aa8699.

[18]. Oettmeier Christina and Döbereiner Hans-Günther. A lumped parameter model of endoplasm flow in Physarum polycephalum explains migration and polarization-induced asymmetry during the onset of locomotion. PLOS ONE, 14(4):e0215622, April 2019. doi: 10.1371/journal.pone.0215622. [PubMed: 31013306]

[19]. Oettmeier Christina, Nakagaki Toshiyuki, and Döbereiner Hans-Günther. Slime mold on the rise: The physics of Physarum polycephalum. Journal of Physics D: Applied Physics, 53(31):310201, May 2020. doi: 10.1088/1361-6463/ab866c.

[20]. Zhang Shun, Guy Robert D., Lasheras Juan C., and del Álamo Juan C.. Self-organized mechano-chemical dynamics in amoeboid locomotion ofPhysarumfragments. Journal of Physics D: Applied Physics, 50(20):204004, April 2017. doi: 10.1088/1361-6463/aa68be. [PubMed: 30906070]

[21]. Zhang Shun, Lasheras Juan C., and del Álamo Juan C.. Symmetry breaking transition towards directional locomotion inPhysarummicroplasmodia. Journal of Physics D: Applied Physics, 52(49):494004, September 2019. doi: 10.1088/1361-6463/ab3ec8.

[22]. Rieu Jean-Paul, Delanoë-Ayari Hélène, Takagi Seiji, Tanaka Yoshimi, and Nakagaki Toshiyuki. Periodic traction in migrating large amoeba of Physarum polycephalum. 12(106):20150099. doi: 10.1098/rsif.2015.0099. URL https://royalsocietypublishing.org/doi/full/10.1098/rsif.2015.0099.

[23]. Lewis Owen L., Zhang Shun, Guy Robert D., and del Álamo Juan C.. Coordination of contractility, adhesion and flow in migrating Physarum amoebae. Journal of The Royal Society Interface, 12(106):20141359, May 2015. doi: 10.1098/rsif.2014.1359. [PubMed: 25904525]

[24]. Finney Tanner J, Parikh Sanjai J, Berman Amir, Sasaki Darryl Y, and Kuhl Tonya L. Characterizing and Tuning the Properties of Polydiacetylene Films for Sensing Applications. Langmuir, page 12, November 2021. doi: 10.1021/acs.langmuir.1c02004.

[25]. Israelachvili J, Min Y, Akbulut M, Alig A, Carver G, Greene W, Kristiansen K, Meyer E, Pesika N, Rosenberg K, and Zeng H. Recent advances in the surface forces apparatus (SFA) technique. Reports on Progress in Physics, 73(3):036601, January 2010. doi: 10.1088/0034-4885/73/3/036601.

[26]. Ananthakrishnan Revathi and Ehrlicher Allen. The Forces Behind Cell Movement. International Journal of Biological Sciences, 3(5):303–317, June 2007. [PubMed: 17589565]

[27]. Luengo Gustavo, Schmitt Franz-Josef, Hill Robert, and Israelachvili Jacob. Thin Film Rheology and Tribology of Confined Polymer Melts: Contrasts with Bulk Properties. Macromolecules, 30(8):2482–2494, April 1997. doi: 10.1021/ma9519122.

[28]. Gourier C, Alba M, Braslau A, Daillant J, Goldmann M, Knobler CM, Rieutord F, and Zalczer G. Structure and Elastic Properties of 10-12 Pentacosadiyonic Acid Langmuir Films. Langmuir, 17(21):6496–6505, October 2001. doi: 10.1021/la001799v.

[29]. Salem Lionel. Attractive Forces between Long Saturated Chains at Short Distances. The Journal of Chemical Physics, 37(9):2100–2113, November 1962. doi: 10.1063/1.1733431.

[30]. Martins José A.. Toward a Physical Definition of Entanglements. Journal of Macro-molecular Science, Part B, 50(4):769–794, February 2011. doi: 10.1080/00222341003785151.

[31]. Huang Xin, Jiang Siguang, and Liu Minghua. Metal Ion Modulated Organization and Function of the Langmuir-Blodgett Films of Amphiphilic Diacetylene: Photopolymerization, Thermochromism, and Supramolecular Chirality. The Journal of Physical Chemistry B, 109(1):114–119, January 2005. doi: 10.1021/jp046500m. [PubMed: 16850992]

[32]. Lifshitz Yevgeniy, Upcher Alexander, Kovalev Anatoly, Wainstein Dmitry, Rashkovsky Alexander, Zeiri Leila, Golan Yuval, and Berman Amir. Zinc modified polydiacetylene Langmuir films. Soft Matter, 7(19):9069–9077, September 2011. doi: 10.1039/C1SM05904A.

[33]. Upcher Alexander, Lifshitz Yevgeniy, Zeiri Leila, Golan Yuval, and Berman Amir. Effect of metal cations on polydiacetylene Langmuir films. Langmuir: the ACS journal of surfaces and colloids, 28(9):4248–4258, March 2012. doi: 10.1021/la204735t. [PubMed: 22288778]

[34]. Wu Si, Pan Libin, Huang Youju, Yang Ni, and Zhang Qijin. Co-assemblies of polydiacetylenes and metal ions for solvent sensing. Soft Matter, 14(33):6929–6937, 2018. doi: 10.1039/C8SM01282B. [PubMed: 30101245]

[35]. Stockem Wilhelm and Brix Klaudia. Analysis of Microfilament Organization and Contractile Activities in Physarum. In Jeon Kwang W. and Jarvik Jonathan, editors, International Review of Cytology, volume 149, pages 145–215. Academic Press, January 1994. doi: 10.1016/S0074-7696(08)62088-4.

[36]. Nakagaki Toshiyuki, Umemura Shoji, Kakiuchi Yasutaka, and Ueda Tetsuo. Action Spectrum for Sporulation and Photoavoidance in the Plasmodium of Physarum polycephalum, as Modified Differentially by Temperature and Starvation. Photochemistry and Photobiology, 64(5):859–862, 1996. doi: 10.1111/j.1751-1097.1996.tb01847.x. [PubMed: 8931386]

[37]. Hato Masakatsu, Ueda Tetsuo, Kurihara Kenzo, and Kobatake Yonosuke. Phototaxis in True Slime Mold Physarum polycephalum. Cell Structure and Function, 1(3):269–278, 1976. doi: 10.1247/csf.1.269.

[38]. Patino-Ramirez Fernando, Arson Chloé, and Dussutour Audrey. Substrate and cell fusion influence on slime mold network dynamics. Scientific Reports, 11(1):1498, January 2021. doi: 10.1038/s41598-020-80320-2. [PubMed: 33452314]

[39]. Brix Klaudia and Stockem Wilhelm. Functional analysis of actin fibrils in Physarum polycephalum. Cell and Tissue Research, 257(1):115–122, July 1989. doi: 10.1007/BF00221640.

[40]. Brix Klaudia, Kukulies J, and Stockem W. Studies on microplasmodia ofPhysarum polycephalum. Protoplasma, 137(2):156–167, June 1987. doi: 10.1007/BF01281151.

[41]. Ohl Christiane, Brix Klaudia, and Stockem Wilhelm. Studies on microplasmodia of Physarum polycephalum. Cell and Tissue Research, 264(2):283–291, May 1991. doi: 10.1007/BF00313965.

[42]. Polacheck William J. and Chen Christopher S.. Measuring cell-generated forces: A guide to the available tools. Nature Methods, 13(5):415–423, May 2016. doi: 10.1038/nmeth.3834. [PubMed: 27123817]

[43]. Bell E, Ivarsson B, and Merrill C. Production of a tissue-like structure by contraction of collagen lattices by human fibroblasts of different proliferative potential in vitro. Proceedings of the National Academy of Sciences, 76(3):1274–1278, March 1979. doi: 10.1073/pnas.76.3.1274.

[44]. Lee J, Leonard M, Oliver T, Ishihara A, and Jacobson K. Traction forces generated by locomoting keratocytes. Journal of Cell Biology, 127(6):1957–1964, December 1994. doi: 10.1083/jcb.127.6.1957. [PubMed: 7806573]

[45]. Maskarinec Stacey A., Franck Christian, Tirrell David A., and Ravichandran Guruswami. Quantifying cellular traction forces in three dimensions. Proceedings of the National Academy of Sciences, 106(52):22108–22113, December 2009. doi: 10.1073/pnas.0904565106.

[46]. Balaban Nathalie Q., Schwarz Ulrich S., Riveline Daniel, Goichberg Polina, Tzur Gila, Sabanay Ilana, Mahalu Diana, Safran Sam, Bershadsky Alexander, Addadi Lia, and Geiger Benjamin. Force and focal adhesion assembly: A close relationship studied using elastic micropatterned substrates. Nature Cell Biology, 3(5):466–472, May 2001. doi: 10.1038/35074532. [PubMed: 11331874]

[47]. Franck Christian, Maskarinec Stacey A., Tirrell David A., and Ravichandran Guruswami. Three-Dimensional Traction Force Microscopy: A New Tool for Quantifying Cell-Matrix Interactions. PLOS ONE, 6(3):e17833, March 2011. doi: 10.1371/journal.pone.0017833. [PubMed: 21468318]

[48]. Butler James P., Tolić-Nørrelykke Iva Marija, Fabry Ben, and Fredberg Jeffrey J.. Traction fields, moments, and strain energy that cells exert on their surroundings. American Journal of Physiology-Cell Physiology, 282(3):C595–C605, March 2002. doi: 10.1152/ajpcell.00270.2001. [PubMed: 11832345]

[49]. Wang Ning, Tolić-Nørrelykke Iva Marija, Chen Jianxin, Mijailovich Srboljub M., Butler James P., Fredberg Jeffrey J., and Stamenović Dimitrije. Cell prestress. I. Stiffness and prestress are closely associated in adherent contractile cells. American Journal of Physiology-Cell Physiology, 282(3):C606–C616, March 2002. doi: 10.1152/ajpcell.00269.2001. [PubMed: 11832346]

[50]. Pelham Robert J. and Wang Yu-li. Cell locomotion and focal adhesions are regulated by substrate flexibility. Proceedings of the National Academy of Sciences, 94(25):13661–13665, December 1997. doi: 10.1073/pnas.94.25.13661.

[51]. Tan John L., Tien Joe, Pirone Dana M., Gray Darren S., Bhadriraju Kiran, and Chen Christopher S.. Cells lying on a bed of microneedles: An approach to isolate mechanical force. Proceedings of the National Academy of Sciences, 100(4):1484–1489, February 2003. doi: 10.1073/pnas.0235407100.

[52]. Fu Jianping, Wang Yang-Kao, Yang Michael T., Desai Ravi A., Yu Xiang, Liu Zhijun, and Chen Christopher S.. Mechanical regulation of cell function with geometrically modulated elastomeric substrates. Nature Methods, 7(9):733–736, September 2010. doi: 10.1038/nmeth.1487. [PubMed: 20676108]

[53]. Trichet Léa, Le Digabel Jimmy, Hawkins Rhoda J., Vedula Sri Ram Krishna, Gupta Mukund, Ribrault Claire, Hersen Pascal, Voituriez Raphaël, and Ladoux Benoît. Evidence of a large-scale

mechanosensing mechanism for cellular adaptation to substrate stiffness. Proceedings of the National Academy of Sciences, 109(18):6933–6938, May 2012. doi: 10.1073/pnas.1117810109.

[54]. du Roure Olivia, Saez Alexandre, Buguin Axel, Austin Robert H., Chavrier Philippe, Siberzan Pascal, and Ladoux Benoit. Force mapping in epithelial cell migration. Proceedings of the National Academy of Sciences, 102(7):2390–2395, February 2005. doi: 10.1073/pnas.0408482102.

[55]. Ghassemi Saba, Meacci Giovanni, Liu Shuaimin, Gondarenko Alexander A., Mathur Anurag, Roca-Cusachs Pere, Sheetz Michael P., and Hone James. Cells test substrate rigidity by local contractions on submicrometer pillars. Proceedings of the National Academy of Sciences, 109(14):5328–5333, April 2012. doi: 10.1073/pnas.1119886109.

[56]. Sasaki Darryl Y., Carpick Robert W., and Burns Alan R.. High Molecular Orientation in Mono- and Trilayer Polydiacetylene Films Imaged by Atomic Force Microscopy. Journal of Colloid and Interface Science, 229(2):490–496, September 2000. doi: 10.1006/jcis.2000.7043. [PubMed: 10985828]

[57]. Staritsyn SN, Mamashin VV, Zakharychev VV, Yaminsky IV, Dubrovin EV, Lomonosov AM, Tverdislov VA, and Yakovenko SA. Mixed monolayers of amphiphile-modified nucleic bases and diynoic acids. I. Phase states at air-water interface and in Langmuir-Blodgett films. Biophysics, 49(4):635–645, 2004.

[58]. Pinkard Henry, Stuurman Nico, Ivanov Ivan E., Anthony Nicholas M., Ouyang Wei, Li Bin, Yang Bin, Tsuchida Mark A., Chhun Bryant, Zhang Grace, Mei Ryan, Anderson Michael, Shepherd Douglas P., Hunt-Isaak Ian, Dunn Raymond L., Jahr Wiebke, Kato Saul, Royer Loïïc A., Thiagarajah Jay R., Eliceiri Kevin W., Lundberg Emma, Mehta Shalin B., and Waller Laura. Pycro-Manager: Open-source software for customized and reproducible microscope control. Nature Methods, 18(3):226–228, March 2021. doi: 10.1038/s41592-021-01087-6. [PubMed: 33674797]

[59]. Edelstein Arthur D., Tsuchida Mark A., Amodaj Nenad, Pinkard Henry, Vale Ronald D., and Stuurman Nico. Advanced methods of microscope control using μManager software. Journal of Biological Methods, 1(2):e10, November 2014. doi: 10.14440/jbm.2014.36. [PubMed: 25606571]

[60]. Schindelin Johannes, Arganda-Carreras Ignacio, Frise Erwin, Kaynig Verena, Longair Mark, Pietzsch Tobias, Preibisch Stephan, Rueden Curtis, Saalfeld Stephan, Schmid Benjamin, Tinevez Jean-Yves, White Daniel James, Hartenstein Volker, Eliceiri Kevin, Tomancak Pavel, and Cardona Albert. Fiji: An open-source platform for biological-image analysis. Nature Methods, 9(7):676–682, July 2012. doi: 10.1038/nmeth.2019. [PubMed: 22743772]

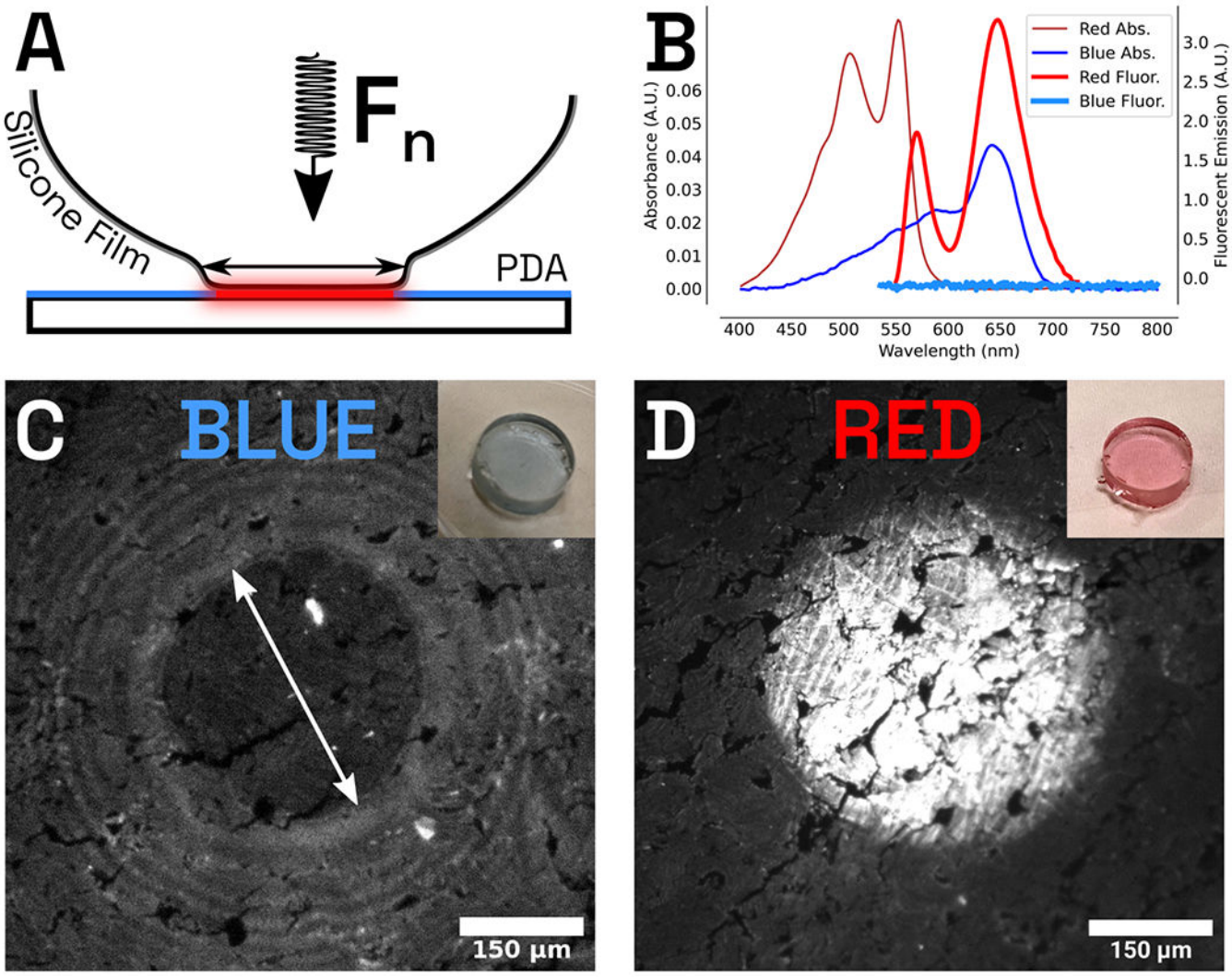

Figure 1:

(A) Schematic of normal stress experiments: films are loaded with well-defined normal forces and the contact area and fluorescent response is measured. The black arrow denotes the contact area diameter. (B) Absorbance and emission spectra of PDA (PCDA) formed on a pure water subphase. (C) Fluorescent micrograph of TCDA (C23) film with edges and pinholes beginning to transform, inset: blue phase of a planar 1 cm SFA disk before loading. The White arrow denotes the contact area diameter. (D) Micrograph of fully transformed TCDA (C23) film from normal stress, inset: red phase of a planar 1 cm SFA disk after macro-scale stress loading.

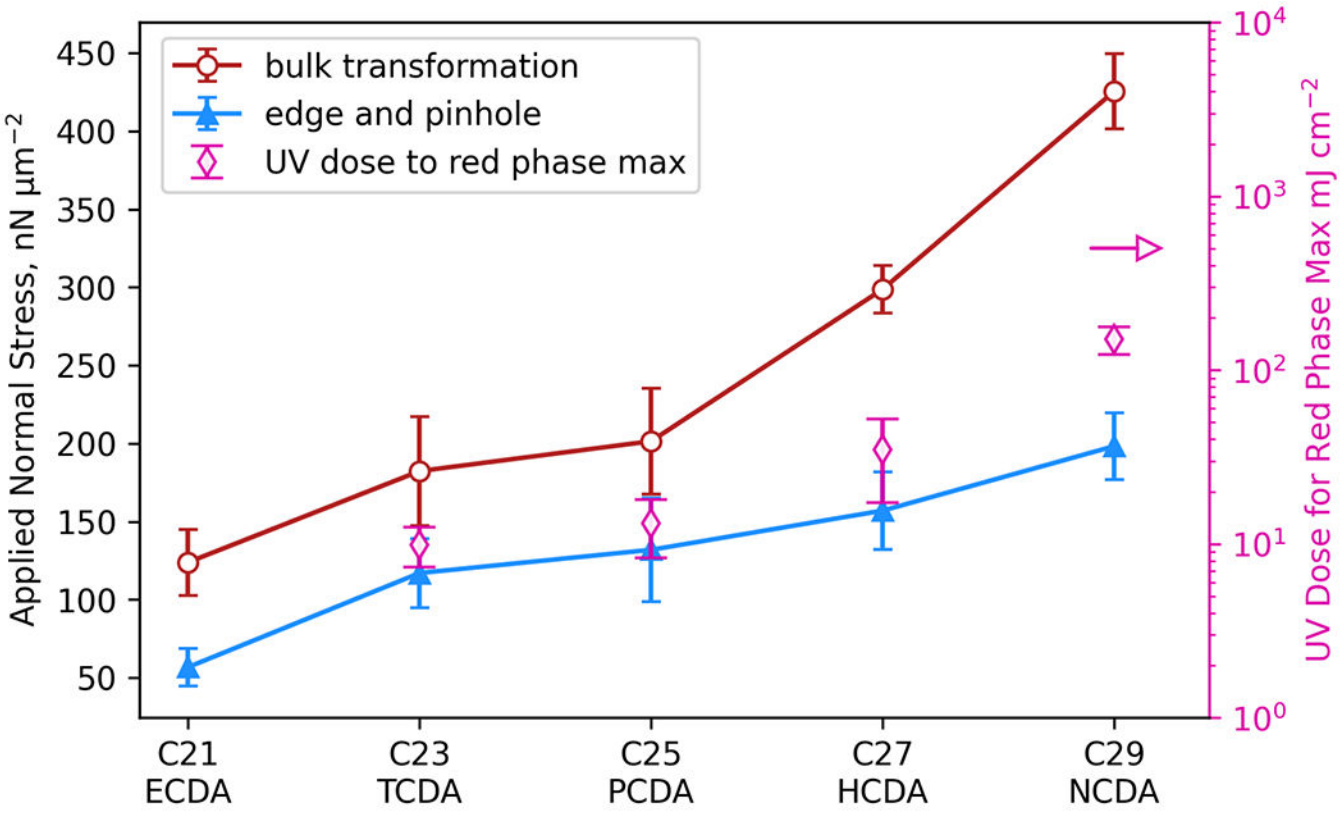

Figure 2:

Critical normal stress required to induce the blue to red transition for PDA films formed from different monomers. UV dose to induce the blue to red transition and produce fully red phase films at the air-water in a Langmuir trough is added for comparison (right axis) [24].

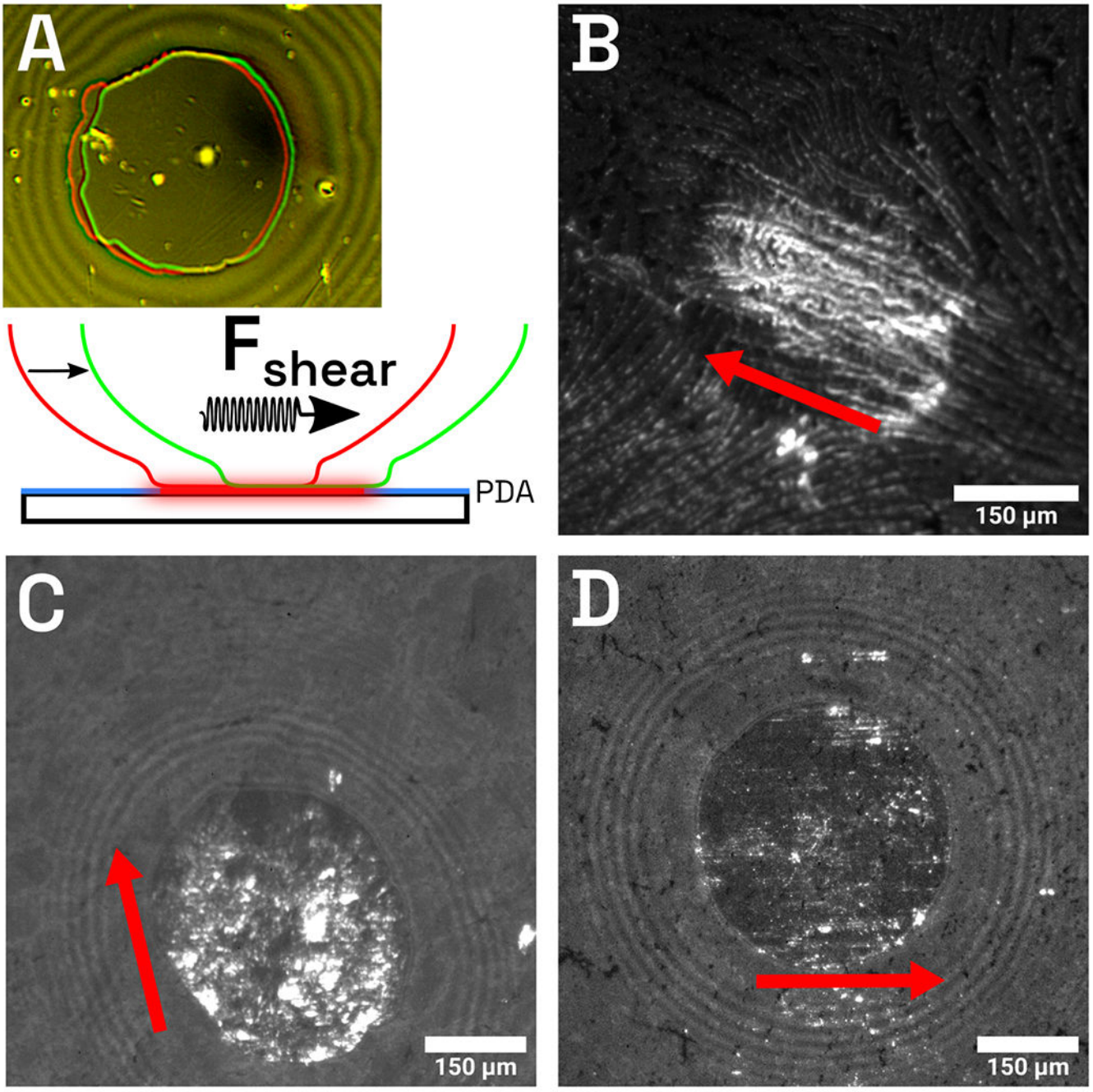

Figure 3:
(A) Schematic of shear stress experiments: a film in contact with a silicone surface is sheared, and the shear force and contact area are measured. Shearing produces a measurable shift in contact area. The red line indicates the initial location of the contact area and the green line indicates the location of the contact area after shearing. Shear induced transitions in films with increasing stress threshold: (B) TCDA/C23, (C) PCDA/C25, (D) NCDA/C29. The red arrow indicates shearing direction.

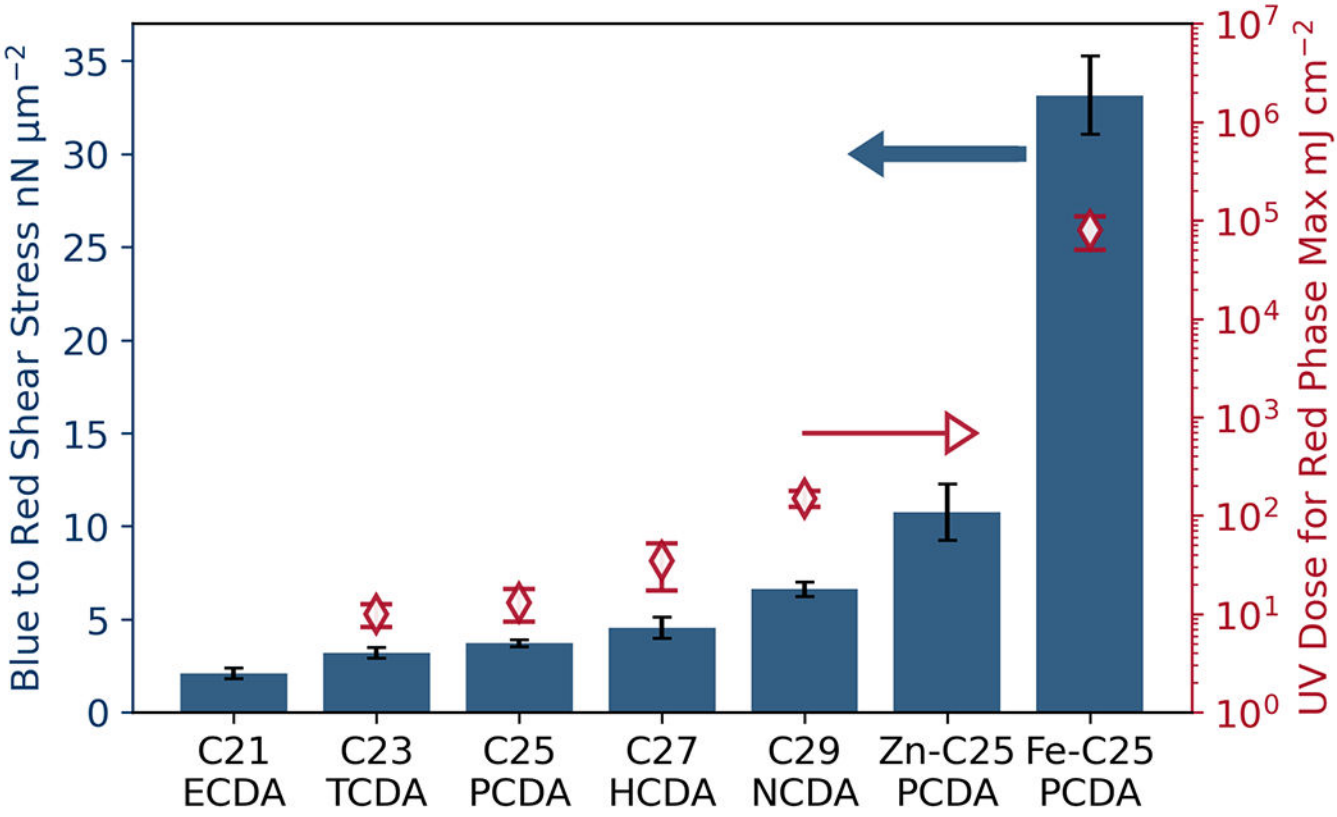

Figure 4:

Critical shear stress required to induce transitions in various PDA films. UV dose to induce the blue to red transition at the air-water interface is added for comparison (right axis), from [24]

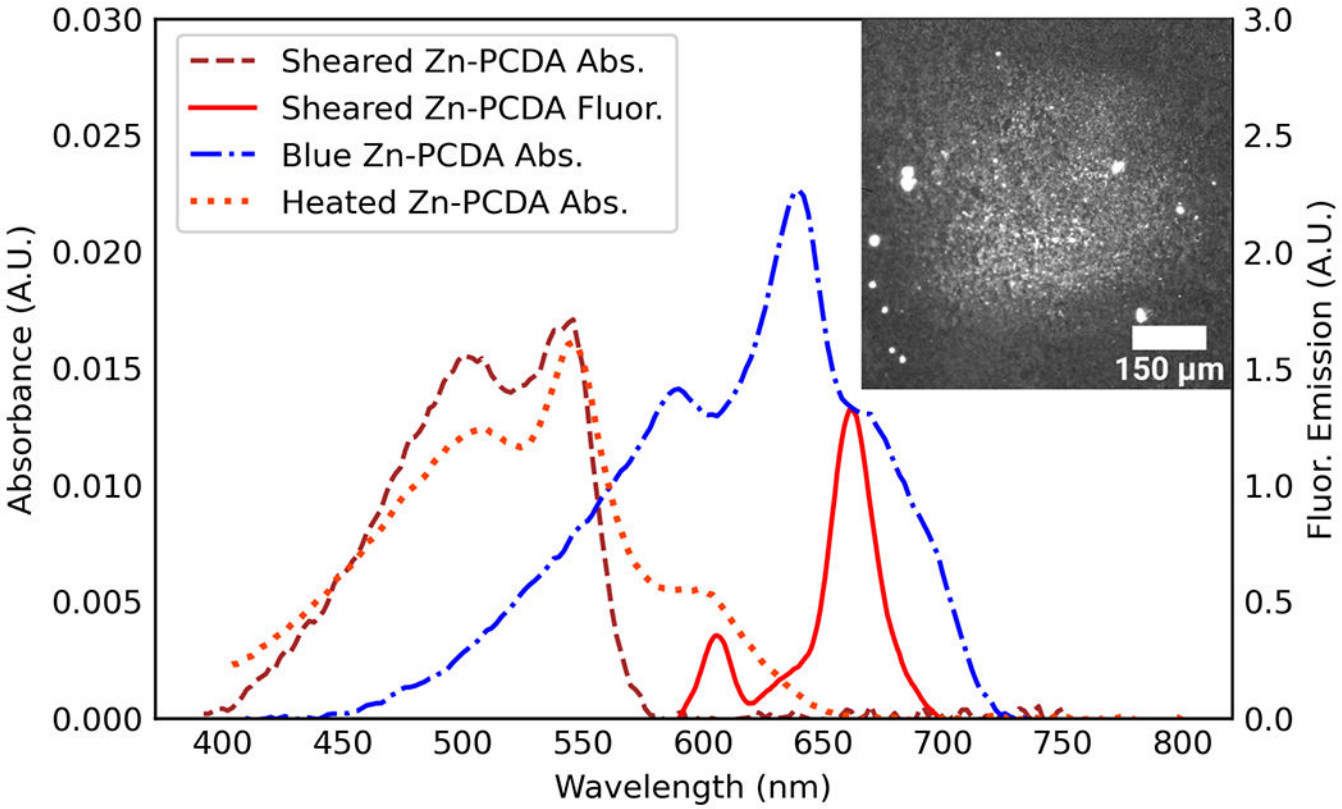

Figure 5:

Absorbance and fluorescent emission spectra of Zn-modified PCDA. Before shearing the film appears visibly blue (Blue Zn-PCDA Abs). Upon heating, the film undergoes appears visibly red, but lacks significant fluorescence (Heated Zn-PCDA Abs). Shearing blue phase Zn-PCDA films induces the blue to red transition and fluorescence (Sheared Zn-PCDA Abs/Fluor). **inset:** Fluorescent micrograph of Zn-PDA film after shearing, scale bar is 150 μm.

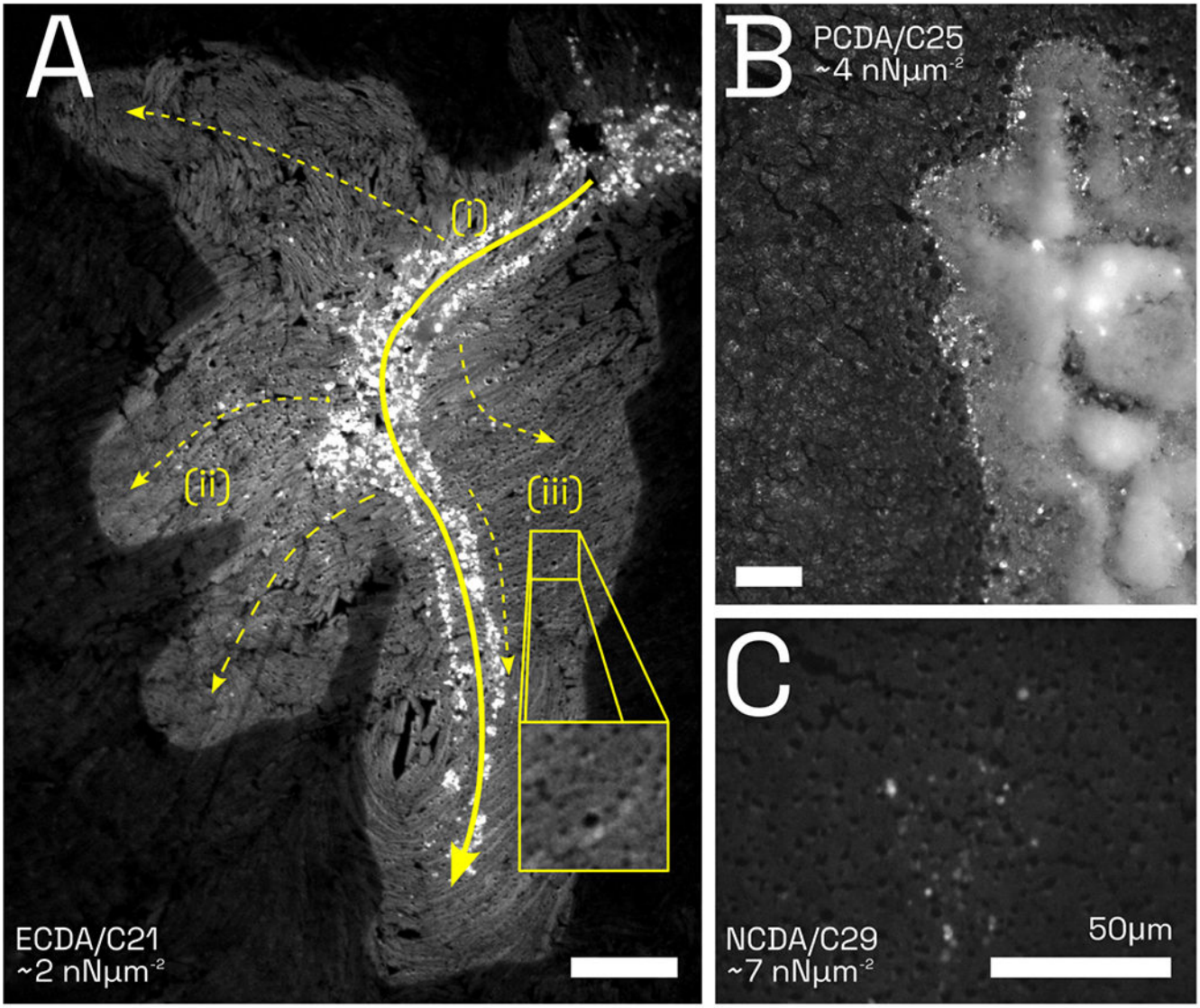

Figure 6:

Fluorescence induced by migration of *Physarum polycephalum* on PDA. Blue to red shear stress (from SFA experiments) is reported for each film system. (A) A variation of fluorescence intensity occurs on a low stress threshold ECDA film. (i) Solid line indicates the primary path of slime mold migration with a high density of fluorescence. (ii) Secondary "exploratory" paths as indicated by more diffuse fluorescence and dashed arrows. (iii) inset highlighting puncta (small dark circular holes) within the slime mold migration region where the PDA film has been removed by the slime mold. (B) Slime mold actively migrating on medium threshold PCDA, puncta and fluorescence can be seen within the slime mold and in the immediate adjacent area. (C) On high threshold NCDA, post migration fluorescence is very low and only localized around puncta and holes. Scale bars are 50μm.

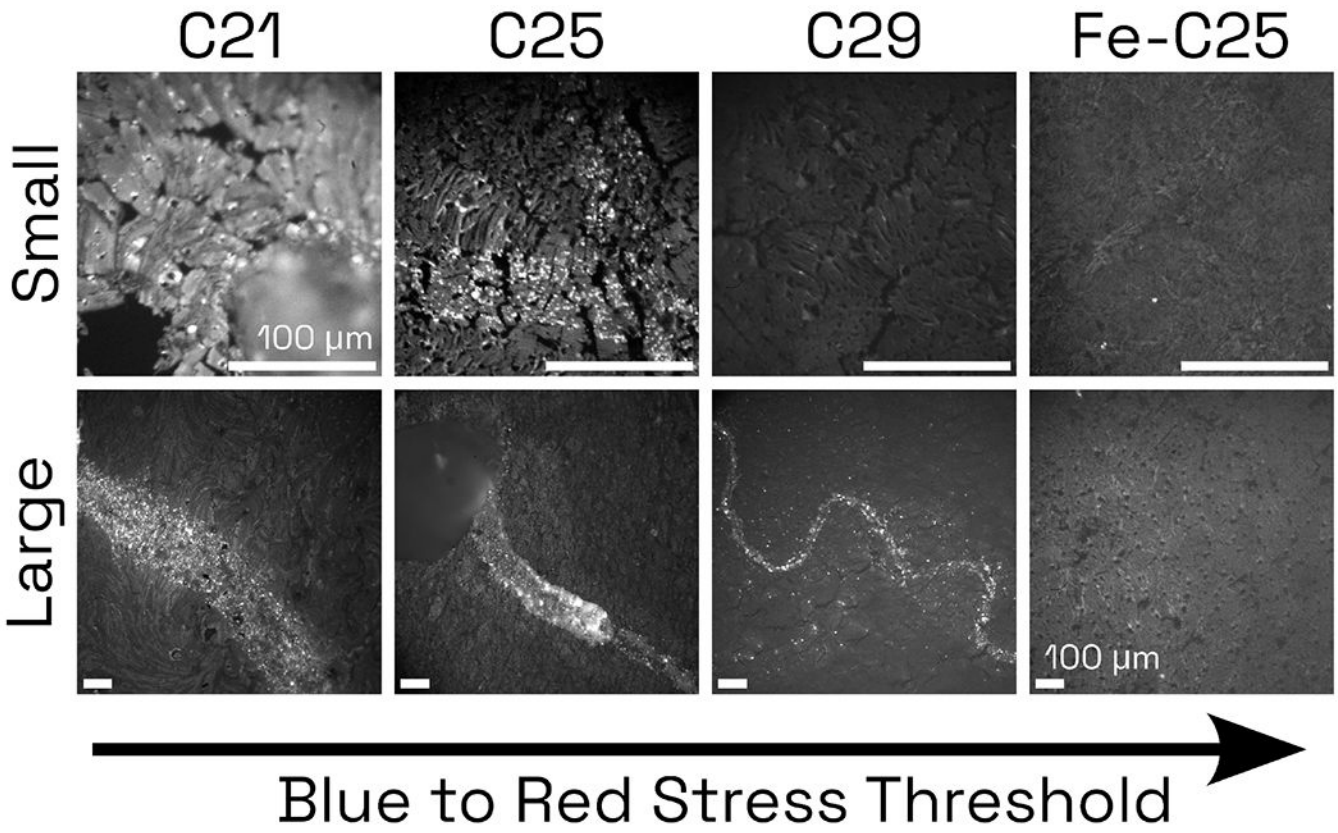

Figure 7:

Relation of slime mold size and film fluorescence on PDA films of increasing blue to red stress threshold. **Top:** Small slime molds (< 100µm) readily transform C21/ECDA (2.1 ± 0.5 nN μm^{-2}), C25/PCDA (3.7 ± 0.2 nN μm^{-2}), but do not transform C29/NCDA (6.7 ± 0.5 nN μm^{-2}) (bright regions), or Fe-C25 (33 ± 2 nN μm^{-2}). No significant puncta are present on Fe-C25. **Bottom:** Fluorescence from larger slime molds > 100µm can be seen in all films except Fe-C25, where only puncta due to removal of the film by the slime mold can be seen.

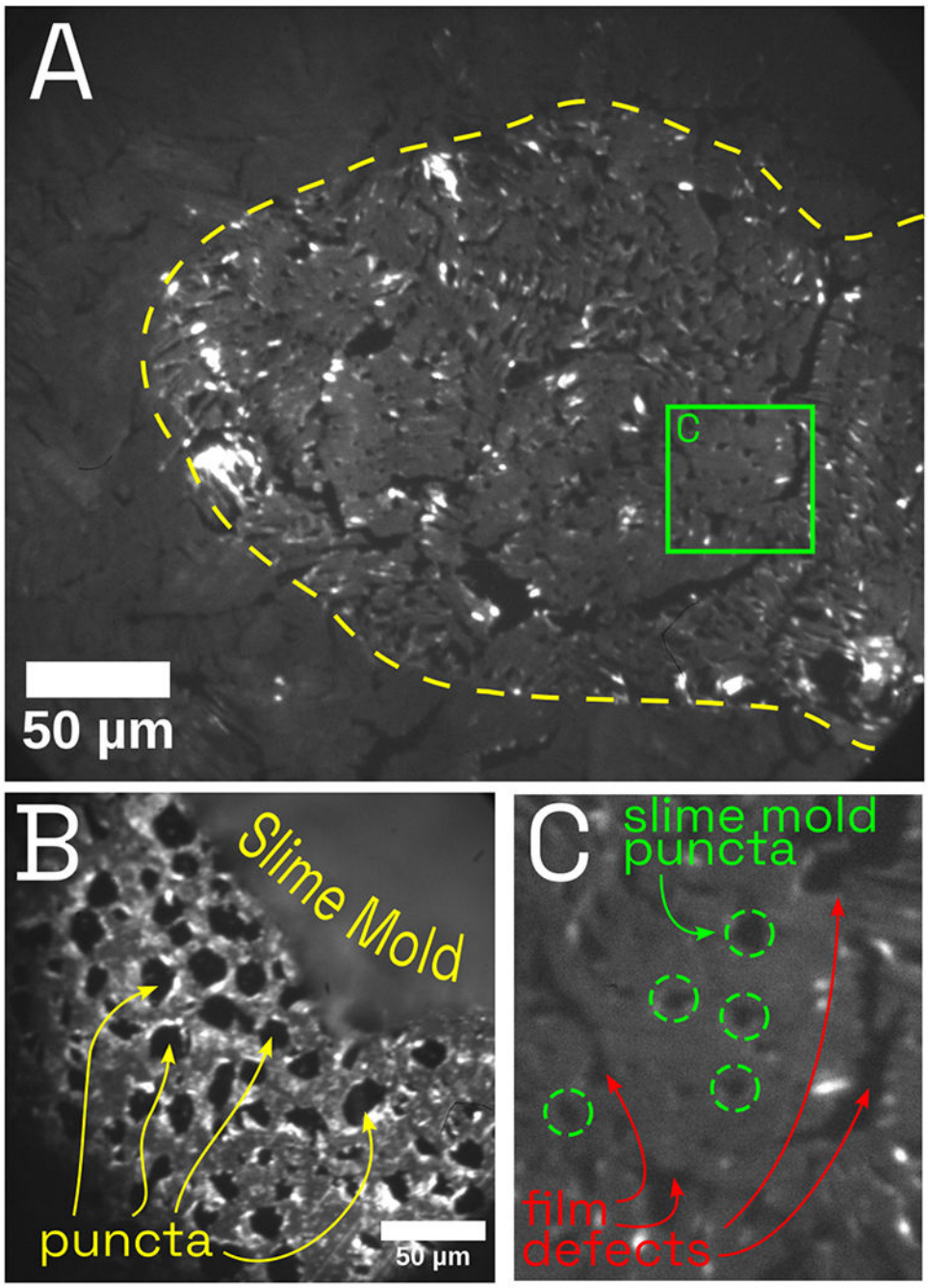

Figure 8:

Comparison of slime mold induced puncta and inherent cracks and defects within a PDA film. (A) PDA film cracks tend to be large and jagged, whereas slime mold puncta are relatively circular, and distributed everywhere within the area that a slime mold migrated. The dashed yellow line shows the extent of slime mold migration. (B) Puncta surrounding a migrating slime mold appear relatively circular, often with a fluorescent halo that we hypothesize was caused by ripping during puncta formation. (C) Zoomed inset comparing select puncta (green circles) to film defects (red arrows).

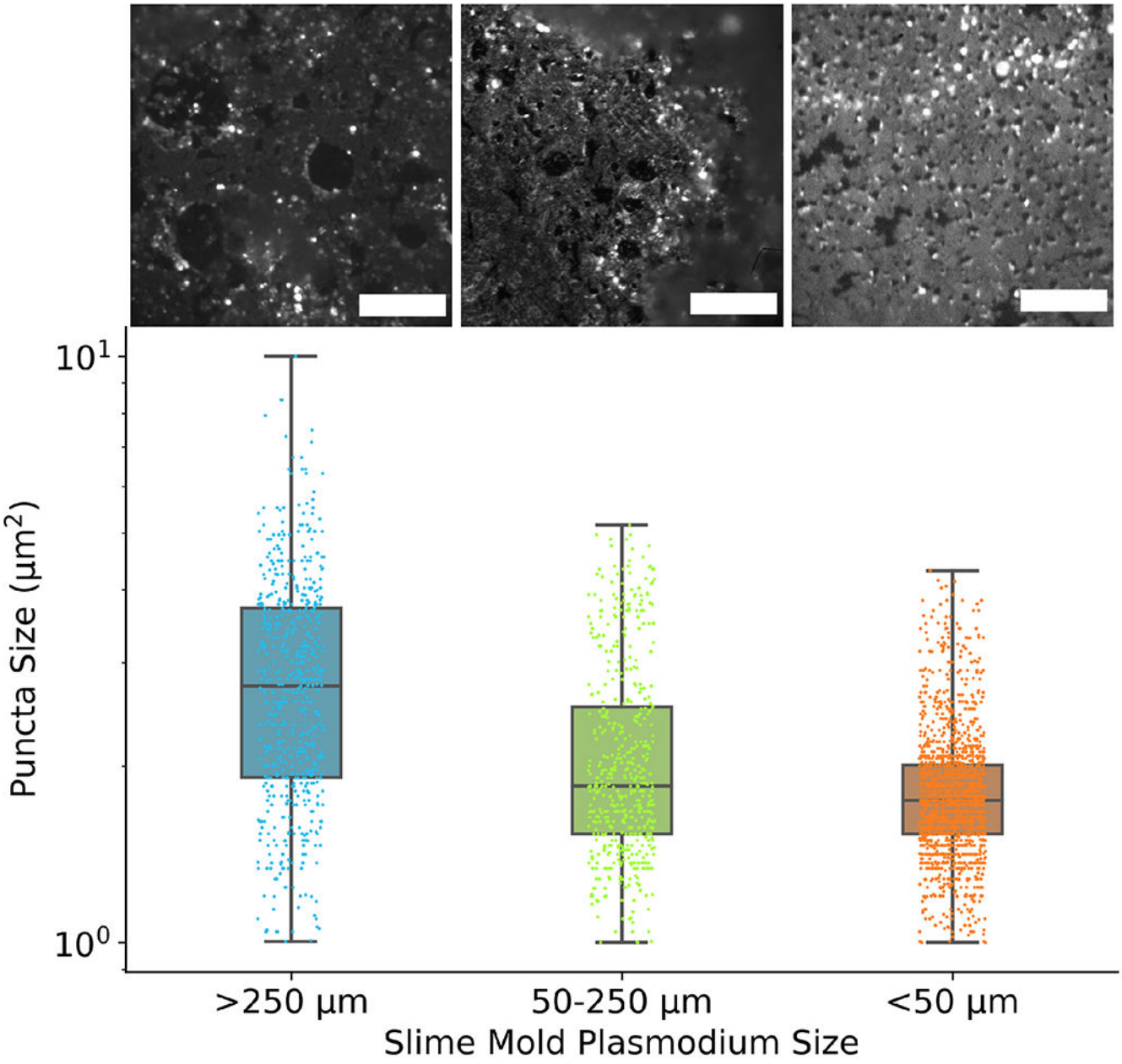

Figure 9:

Relation of slime mold size to measured punctate areas. Above each slime mold size category is an exemplar image of corresponding puncta. Scale bar is 50μm.

Table 1:

Comparison of PDA thin-flims to other well-established techniques for measuring cellular forces. Table adapted from Polacheck and Chen [42].

Technique	Stress range	Number of cells	Spatial resolution[a]	Substrate and stiffness	Special requirements	Strengths	Major limitations	References
Collagen Gel	N/A	1×10^4 to 1×10^6	N/A	Young's modulus: 0.01-0.1 kPa	None	Ease of Implementation	Qualitative, cannot determine stress from single cells	[42, 43]
Traction Force Microscopy	0.05-0.6 kPa	1 to 1000	2 μm	Collagen, PEG, PDMS or PA Young's modulus: 1.2-1000 kPa	Hydrogel, PDMS synthesis & functionalization, particle tracking algorithms	Standard laboratory equipment and fluorescent microscopy	2-D, synthetic substrate	[42, 44, 45, 46, 47, 48, 49, 50]
Micro-pillars	0.06-8 kPa	1-10	1 μm	Collagen or PDMS, pillar stiffness 1.9-1556 nN μm^{-1}	microfabrication, PDMS functionalization	Ease of implementation and computation	Fabrication, Forces are independent for posts	[42, 51, 52, 53, 54, 55]
Polydiacetylenes (PDA)	~2-30 kPa	1-1000s[b]	>μm[c]	Glass[d]	PDA films	Inexpensive, passive, precalibratred, permanent fluorescence, binary stress threshold	2-D, binary transition, cytotoxicity not evaluated, others substrates not evaluated	This Work, [2, 10, 12, 14, 56]

[a] The minimum distance between which two point forces can be resolved.

[b,c,d] See text for details.